Single-Molecule Magnets: Ligand-Induced Core Distortion and Multiple Jahn−Teller Isomerism in $[Mn_{12}O_{12}(O_2CMe)_8(O_2PPh_2)_8(H_2O)_4]$

Colette Boskovic,[†] Maren Pink,[†] John C. Huffman,[†] David N. Hendrickson,*[,‡] and George Christou*[,†,§]

Department of Chemistry and the Molecular Structure Center, Indiana University Bloomington, Indiana 47405-7102
Department of Chemistry-0358 University of California at San Diego La Jolla, California 92093-0358

Received June 4, 2001

Single-molecule magnets (SMMs) are a relatively recent discovery that promises access to the ultimate high-density memory storage device in which each bit of digital information is stored on a single molecule. Each independent molecule of a SMM possesses the ability to function as a magnetizable magnet below a critical temperature.[1] This is due to intrinsic intramolecular properties, that is, a large spin ground state and a large and negative (easy-axis-type) magnetoanisotropy, rather than to intermolecular interactions and long-range ordering. The most well studied SMMs are the $[Mn_{12}O_{12}(O_2CR)_{16}(H_2O)_x]^{n-}$ ($n = 0-2$; $8Mn^{III}4Mn^{IV}$ for $n = 0$) complexes.[2−4] Evidence for the SMM behavior comes from frequency-dependent out-of-phase AC susceptibility signals (χ_M'') and magnetization hysteresis loops. In addition, oriented crystals display steps in the hysteresis loops indicative of field-tuned quantum tunneling of the magnetization (QTM).[5] A substantial amount of effort has been dedicated to systematic variation of the carboxylate R group and solvate molecules of crystallization, which has recently led to the discovery of Jahn−Teller (JT) isomerism,[6] involving differing relative orientations of the JT elongation axes of the eight Mn^{III} centers and resulting in significantly different magnetic behavior for the different JT isomers. This includes differing positions of the χ_M'' peaks and differing magnetization hysteresis plots, both reflecting different rates of magnetization relaxation.

We report herein a major expansion of the Mn_{12} SMM family by demonstrating for the first time that carboxylate ligands can be replaced by other organic ligands, in this case diphenylphosphinate groups to give $[Mn_{12}O_{12}(O_2CMe)_8(O_2PPh_2)_8(H_2O)_4]$. In addition, this species is unique in displaying three distinct JT isomers, two of which cocrystallize in the same crystal.

The reaction of $[Mn_{12}O_{12}(O_2CMe)_{16}(H_2O)_4]\cdot 2MeCO_2H\cdot 4H_2O$ (**1**) with 8 equiv of Ph_2PO_2H in MeCN leads to crystallization of $[Mn_{12}O_{12}(O_2CMe)_8(O_2PPh_2)_8(H_2O)_4]$ (**2**) in 60% yield, which was crystallographically characterized as $\mathbf{2}\cdot{}^{14}/_{3}MeCN\cdot{}^{4}/_{3}H_2O$.[7] Recrystallization from CH_2Cl_2/hexanes gives $\mathbf{2}\cdot 12CH_2Cl_2$.[8] $\mathbf{2}\cdot{}^{14}/_{3}MeCN\cdot{}^{4}/_{3}H_2O$ crystallizes in space group $C2/c$ with two independent molecules, the asymmetric unit containing 1.5 Mn_{12} clusters in addition to solvent. $\mathbf{2}\cdot 12CH_2Cl_2$ crystallizes in space group $P4_2/n$, with the asymmetric unit containing 0.25 Mn_{12} clusters and solvent. All three crystallographically unique molecules possess a structure similar to that of **1**, with a central $[Mn^{IV}_4O_4]$ cubane held within a nonplanar ring of eight Mn^{III} ions by eight μ_3-O^{2-} ions. However, in **2** the acetate groups at the four axial $Mn^{III}-Mn^{III}$ and four of the eight equatorial $Mn^{III}-Mn^{III}$ carboxylate sites have been replaced by diphenylphosphinate groups, while the remaining equatorial sites and the four axial $Mn^{IV}-Mn^{III}$ sites remain occupied by acetates (Figure 1), resulting in a significant distortion of the $[Mn_{12}O_{12}]^{16+}$ core (Figure 2). This is reflected in the bond angles and an increase of ∼0.1 Å in all of the $Mn^{III}-Mn^{III}$ distances in **2**, and is most apparent as a "bowing" in each of the linear Mn_4 units, with the angles of the type Mn(3)−Mn(1)−Mn(1′) in $\mathbf{2}\cdot 12CH_2Cl_2$ decreasing from ∼178° in **1** to 171−173° in **2**. All three of the molecules possess one H_2O ligand bound to every other Mn^{III} center (Mn(2) for $\mathbf{2}\cdot 12CH_2Cl_2$), oriented alternately in opposite directions, as is observed in **1**. The main difference between the three different molecules of **2** lies in the location of the JT elongation axes of the eight Mn^{III} centers (Figure 2). The single cluster in $\mathbf{2}\cdot 12CH_2Cl_2$ possesses S_4 symmetry with all eight JT axes oriented approximately parallel in the axial direction, and thus they are not pointing toward the oxide ligands. This is the same as in **1** and is the normal situation in Mn_{12}-carboxylate species. However, the two independent molecules in $\mathbf{2}\cdot{}^{14}/_{3}MeCN\cdot{}^{4}/_{3}H_2O$ possess C_1 and approximate S_4 (crystallographic C_2) symmetry, with two

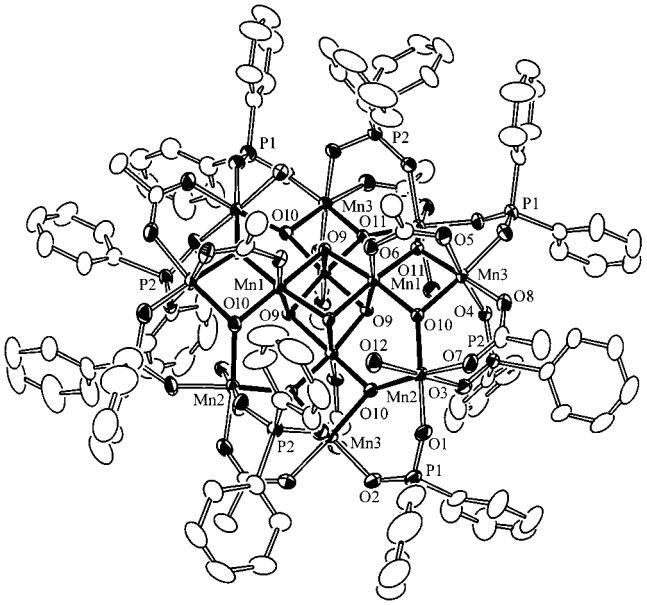

Figure 1. ORTEP representation of complex $\mathbf{2}\cdot 12CH_2Cl_2$ at the 50% probability level.

[†] Indiana University.
[‡] University of California at San Diego.
[§] Present address: Department of Chemistry, University of Florida, Gainesville, FL 32611-7200.

(1) Christou, G.; Gatteschi, D.; Hendrickson, D. N.; Sessoli, R. *MRS Bulletin* **2000**, *25*, 66.
(2) (a) Sessoli, R.; Tsai, H.-L.; Schake, A. R.; Wang, S.; Vincent, J. B.; Folting, K.; Gatteschi, D.; Christou, G.; Hendrickson, D. N. *J. Am. Chem. Soc.* **1993**, *115*, 1804. (b) Sessoli, R.; Gatteschi, D.; Caneschi, A.; Novak, M. A. *Nature* **1993**, *365*, 141.
(3) (a) Eppley, H. J.; Tsai, H.-L.; de Vries, N.; Folting, K.; Christou, G.; Hendrickson, D. N. *J. Am. Chem. Soc.* **1995**, *117*, 301. (b) Aubin, S. M. J.; Sun, Z.; Pardi, L.; Krzystek, J.; Folting, K.; Brunel, L.-C.; Rheingold, A. L.; Christou, G.; Hendrickson, D. N. *Inorg. Chem.* **1999**, *38*, 5329.
(4) Soler, M.; Chandra, S. K.; Ruiz, D.; Davidson, E. R.; Hendrickson, D. N.; Christou, G. *Chem. Commun.* **2000**, 2417.
(5) (a) Friedman, J. R.; Sarachik, M. P.; Tejada, J.; Maciejewski, J.; Ziolo, R. *J. Appl. Phys.* **1996**, *79*, 6031. (b) Thomas, L.; Lionti, F.; Ballou, R.; Gatteschi, D.; Sessoli, R.; Barbara, B. *Nature* **1996**, *383*, 145.
(6) (a) Sun, Z.; Ruiz, D.; Dilley, N. R.; Soler, M.; Ribas, J.; Folting, K.; Maple, M. B.; Christou, G.; Hendrickson, D. N. *Chem. Commun.* **1999**, 1973. (b) Aubin, S. M. J.; Sun, Z.; Eppley, H. J.; Rumberger, E. M.; Guzei, I. A.; Folting, K.; Gantzel, P. K.; Rheingold, A. L.; Christou, G.; Hendrickson, D. N. *Inorg. Chem.* **2001**, *40*, 2127.

(7) Crystal data for $^{3}/_{2}[\mathbf{2}]\cdot 7MeCN\cdot 2H_2O$: $C_{182}H_{193}N_7Mn_{18}O_{74}P_{12}$, 5023.11 g mol^{-1}, monoclinic, $C2/c$, $a = 55.071(4)$ Å, $b = 33.491(3)$ Å, $c = 27.331(2)$ Å, $\beta = 114.966(2)°$, $Z = 8$, $V = 45699.0$ Å^3, $d_{calc} = 1.460$ g cm^{-3}, $T = -158$ °C. The structure was solved by direct methods (SHELXTL) and refined (on F) using 52 187 reflections with $F > 3\sigma(F)$ to $R(R_w)$ values of 0.0777 (0.0645).

(8) Crystal data for $\mathbf{2}\cdot 12CH_2Cl_2$: $C_{124}H_{136}Cl_{24}Mn_{12}O_{48}P_8$, 4152.17 g mol^{-1}, tetragonal, $P4_2/n$, $a = b = 25.208(2)$ Å, $c = 13.413(1)$ Å, $Z = 2$, $V = 8523.1$ Å^3, $d_{calc} = 1.618$ gcm^{-3}, $T = -160$ °C. The structure was solved by direct methods (SHELXTL) and refined (on F) using 9776 reflections with $F > 2\sigma(F)$ to $R(R_w)$ values of 0.0666 (0.2180).

10.1021/ja016341+ CCC: $20.00
Published on Web 09/14/2001

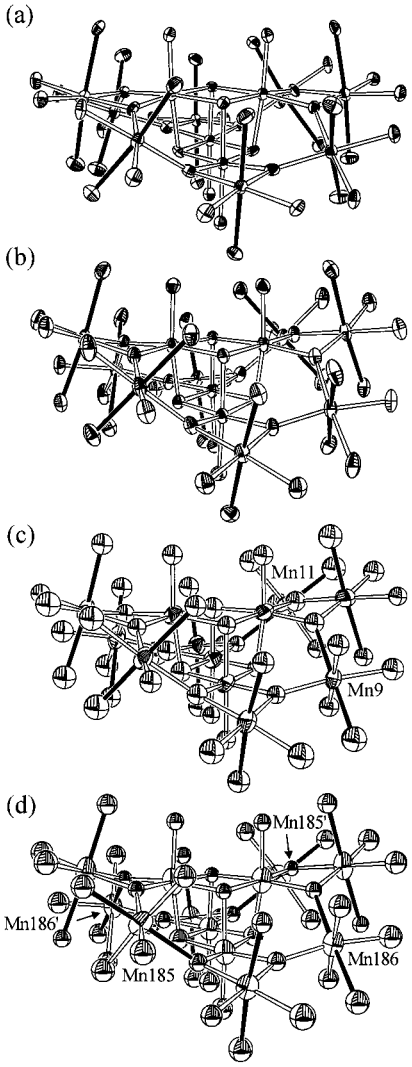

Figure 2. The cores of complexes: (a) **1**, (b) **2**·12CH_2Cl_2, (c) the C_1 molecule of **2**·14/3MeCN·4/3H_2O, and (d) the C_2 molecule of **2**·14/3MeCN·4/3H_2O, emphasizing the Jahn−Teller axes as solid black bonds.

(Mn(9) and Mn(11)) and four (Mn(185), Mn(185′), Mn(186), and Mn(186′)) equatorially oriented JT axes, respectively. That is, for these species, some of the JT axes point toward oxide ligands. In both cases, these "abnormally" oriented JT axes are located at the Mn^{III} centers with H_2O ligands, as has been observed for the previously reported examples of JT isomerism.[6]

The ground state of **2**·12CH_2Cl_2 was determined from reduced magnetization ($M/N\mu_B$) versus H/T measurements in the 1.8−25 K and 20−70 kG range.[9] Fitting of the data[10] gave $S = 10$, $g = 1.92$ and $D = -0.41$ cm^{-1} (−0.59 K), values typical for $[Mn_{12}O_{12}(O_2CR)_{16}(H_2O)_x]$ clusters ($S = 10$, $D = -0.4$ to -0.5 cm^{-1}).

AC magnetization measurements were performed on **2**·12CH_2Cl_2 in the 1.8−10 K range in a 3.5 G AC field oscillating at 1−1500 Hz. The in-phase $\chi_M'T$ signal shows a frequency-dependent decrease at $T < 8$ K, indicative of the onset of slow relaxation. This was confirmed by the concomitant appearance

(9) See Supporting Information.

(10) Vincent, J. B.; Christmas, C.; Chang, H.-R.; Li, Q.; Boyd, P. D. W.; Huffman, J. C.; Hendrickson, D. N.; Christou, G. *J. Am. Chem. Soc.* **1989**, *111*, 2086.

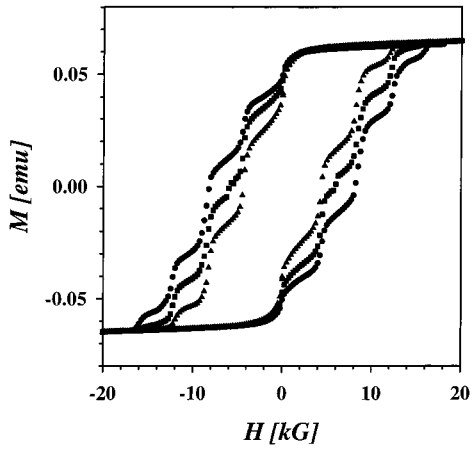

Figure 3. Magnetization hysteresis loops for oriented crystals measured in an eicosane matrix for complex **2**·12CH_2Cl_2 at 1.8 (●), 1.9 (■), and 2.0 K (▲).

of an out-of-phase (χ_M'') signal due to the inability of **2**·12CH_2Cl_2 to relax sufficiently rapidly at these temperatures to keep up with the oscillating field. For the AC frequency range 1−1500 Hz, the χ_M'' peaks of **2**·12CH_2Cl_2 occur in the range 3−7 K, again consistent with the behavior generally observed for $[Mn_{12}O_{12}(O_2CR)_{16}(H_2O)_x]$. The χ_M'' data obtained by varying the oscillation frequency of the AC field can be fit to an Arrhenius equation to give the effective energy barrier for the magnetization relaxation (U_{eff}),[9] and such an analysis indicates that U_{eff} for complex **2**·12CH_2Cl_2 is ∼42 cm^{-1} (60 K), which again is within the normal range for $[Mn_{12}O_{12}(O_2CR)_{16}(H_2O)_x]$ of 42−50 cm^{-1} (60−72 K). AC measurements on **2**·14/3MeCN·4/3H_2O are in progress, but are hindered by crystal degradation following rapid solvent loss.

Magnetization hysteresis loops were observed for oriented crystals of **2**·12CH_2Cl_2 at 1.8, 1.9, and 2.0 K (Figure 3). A few crystals were suspended in eicosane at 40 °C, subjected to a 70 kG field to align their principal axis of magnetization parallel to the applied field, and then cooled to low temperature. A number of steps due to quantum tunneling of the magnetization are evident in the hysteresis loop. The separation between steps was found to be 3.95 kG, indicating a value of D/g of ∼−0.18 cm^{-1}, which is consistent with the value of −0.21 cm^{-1} obtained from the fitting of the reduced magnetization data.

In conclusion, the first significantly altered derivative of $[Mn_{12}O_{12}(O_2CR)_{16}(H_2O)_x]$ has been prepared by incorporation of non-carboxylate organic ligands, and ligand-induced core distortions result. In addition, multiple JT isomerism has been observed, emphasizing the small energy differences involved. Complex **2** is magnetochemically similar to its 16-carboxylate parent, possessing an $S = 10$ ground state and displaying frequency-dependent peaks in the out-of-phase AC susceptibility plots, in addition to magnetization hysteresis. Furthermore, quantum tunneling of the magnetization is evident as steps in the hysteresis loops. Therefore, the SMM properties are still retained in the diphenylphosphinate-substituted species **2**, which thus represents the prototype of a major new thrust in the SMM field.

Acknowledgment. This work was supported by National Science Foundation grants to G.C. and D.N.H.

Supporting Information Available: Crystallographic details (CIF) for **2**·12CH_2Cl_2 and **2**·14/3MeCN·4/3H_2O; reduced magnetization versus field plots and fit; Arrhenius plot. This material is available free of charge via the Internet at http://pubs.acs.org.

JA016341+